JOURNAL OF COMPUTATIONAL PHYSICS 14, 59–83 (1974)

A Uniform Vector Distribution for Accurate Spatial Integration*

W. C. OVERTON, JR., AND A. F. SCHUCH

Los Alamos Scientific Laboratory, University of California, Los Alamos, New Mexico 87544

Received June 21, 1973

A method is developed for the design of exactly uniform high-density vectorial distributions inside the 1/48th symmetry-irreducible trihedral angle of highest cubic symmetry. The first application led to a particular 489-vector distribution in the basic solid angle which extends, by permutations, to 23,472 uniformly-distributed vectors in the full 4π steradians. This density ($N = 489$) meets a criterion of about one part in 10^5 set for the accuracy requirement of three-dimensional integration of functions in crystal lattice dynamics and in elastic wave theory. The dependence of the accuracy of numerical calculations on vector density is determined by comparison with exact integrals of certain octahedral functions. It is found to depend significantly on the three-dimensional anisotropy of the surfaces of these functions. A ten-decimal table of the direction cosines of the 489-vector distribution is supplied as an appendix.

I. INTRODUCTION

The theory of lattice vibrations of a crystal solid leads to the prescription of a very large number rN_0 of eigenfrequencies of the form $\nu_p(\mathbf{q}_i)$. Here $p = 1, 2, 3,..., r$ ($r = 3 \times$ number of atoms per lattice unit cell) and $i = 1,..., N_0$ ($\sim$Avagadro number) points $\mathbf{q}_i$ in the reciprocal lattice space of the Brillouin zone [1]. In principle, in the harmonic approximation, all of the thermodynamic properties of a crystal are calculable from the Helmholtz free energy in the form

$$F = \Phi + \sum_p^{3r} \sum_i^{N_0} (\tfrac{1}{2}h\nu_p(\mathbf{q}_i) + kT \ln\{1 - \exp[-h\nu_p(\mathbf{q}_i)/kT]\}),$$

where Φ is the static lattice potential energy. In practice, it is impossible to perform such a summation over 10^{24} points. However, since the $\mathbf{q}_i$ are so densely distributed and functions defining $\nu(\mathbf{q})$ are uniform, one can use the continuum representation in which one replaces the sum for F by an integral weighted by a frequency distribution function $G(\nu)$ (or vibration spectrum or phonon spectrum). Now F becomes in practice an approximate F. The accuracy of one of the theoretical thermo-

* Work performed under the auspices of the U. S. Atomic Energy Commission.

dynamic quantities derivable from F now hinges on the accuracy with which $G(\nu)$ has been determined.

Even the computation of $G(\nu)$ versus ν used to be a formidable task. After prodigious labor one was able to obtain accuracies of only a few percent. (See early works cited in Ref. [1], for example). With modern computers, accuracies of parts in 10^8 are possible. One need not set a goal this high. Actually, the computational accuracy needs only to be one or two orders better than the accuracy of modern experimental measurements. At the present time, six-figure accuracy is quite a reasonable goal and is very much better than the accuracies of a few percent obtainable only a few years ago.

The root-sampling method [1] for calculating a phonon spectrum $G(\nu)$ versus ν for $0 < \nu \leqslant \nu_m$ (ν_m = model maximum) involves solving the dynamical matrix

$$| D_{ij}(\mathbf{q}) - \delta_{ij}\nu^2 | \tag{1.1}$$

at a large number of selected points $\mathbf{q}$'s in the Brillouin zone. The vibrational eigenfrequencies $\nu_p(\mathbf{q})$'s so obtained are sorted into histogram intervals. The details of the method used then determines whether one obtains a good or a poor approximation to the correct curve of $G(\nu)$ versus ν. In (1.1) D_{ij} ($\mathbf{q}$) is a sine–cosine series of terms over shells s of atoms surrounding one chosen as origin [2]. The arguments are $sh\pi aX(q_x, q_y, q_z)$ where h is a proper integer and a is the crystal lattice constant. The coefficients in $D_{ij}(\mathbf{q})$ are the generalized-force interatomic force constants (AFC's) α_i^s, β_j^s[2].

Once $G(\nu)$ versus ν has been obtained, the theoretical thermodynamic properties of a crystal can be calculated easily. A comparison between theory and thermodynamic experimental data then provides one method of testing the validity of the choice of the set $\{\alpha_i^s, \beta_j^s\}$ of AFC's. Unfortunately, the test itself is seldom valid unless $G(\nu)$ versus ν is known with reasable accuracy.

One of the sensitive tests of a phonon model is that of comparing the theoretical and experimental specific heats at low temperatures because here, the specific heat is changing most rapidly as T^3. However, the dominant frequencies in the low T range are the low $\nu(\mathbf{q})$ which correspond to the small values of $\mathbf{q}$ near the origin of the Brillouin zone. Thus, reliable model testing requires very accurate $G(\nu)$ versus ν in this low-ν range.

It is just in the low $\mathbf{q}$ range that the root-sampling method (i.e., roots $\nu_p(\mathbf{q})$ evaluated on some cubic lattice of points) gives the least accurate $G(\nu)$ data. Even when one selects the order of 10^6 points ($\mathbf{q}$'s) in say 1/8th the Brillouin zone, the $G(\nu)$ obtained by conventional root-sampling still may be too crude for valid model testing at low temperatures.

A more reliable method, especially for the low-ν range, has been termed the vector-interpolation method (see Section II below). This method is capable of giving $G(\nu)$ with five- to eight-decimal accuracy (at least for small ν) with only about 50,000 points in 1/48th the zone.

One of the earliest suggestions of the use of the vector method in lattice-dynamics applications seems to be due to Houston [3]. This idea has been extended by de Launay [4] and used in the preparation of tables of Debye θ_D functions for cubic crystals; de Launay used a 69-vector distribution which is hardly different from the 70-vector distribution of Fig. 1a. The latter was used in the 1950's in some

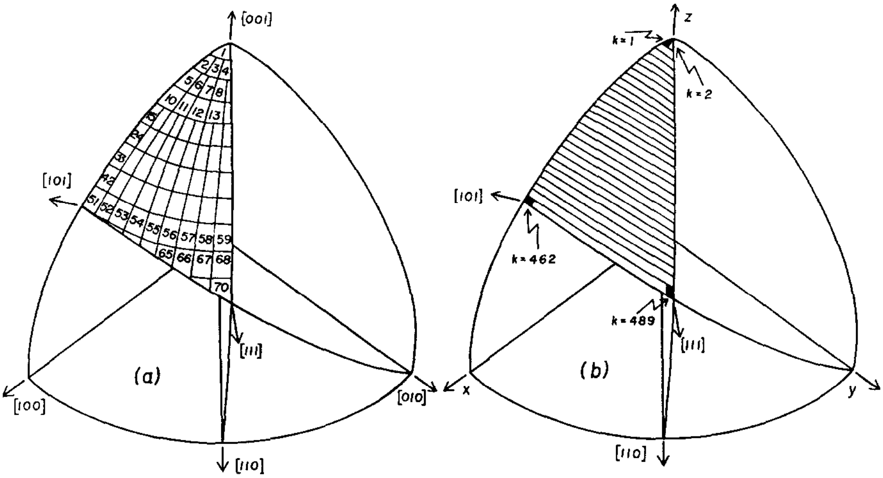

FIG. 1. A typical 1/48th symmetry-irreducible trihedral solid angle segment of the sphere. Spherical coordinates r, θ, ϕ are defined with respect to Cartesian axes x, y, z which we also identify with cubic crystallographic axes [100], [010] and [001], respectively. Fig. (1a): subdivision in 70 unequal surface elements. Fig. (1b): Uniform subdivision of 489 exactly equal elements.

early phonon spectra calculations [5, 6]. Even the 70-vector distribution of Fig. 1a does not provide the accuracy required for testing phonon models except in the unlikely case of nearly spherical surfaces of constant $\nu(\mathbf{q})$. Moreover, the solid angle elements $\Delta\omega$'s surrounding the vectors of Fig. 1a are unequal; obviously, this necessitates a separate weighting factor for each vector.

One purpose of this paper is to-outline the procedure for designing an N-vector distribution of fairly large N for which all vectors have the same weighting factor. This procedure has been applied in designing a distribution with $N = 489$ [7] within the 1/48th symmetry-irreducible trihedral angle of highest cubic symmetry. This segment represents the irreducible spatial subset of octahedral Group $\mathcal{O}$ [8]. We have found that the N-489 distribution satisfies the five- to ten-decimal accuracy criterion for the long wave limit of lattice dynamics. Accordingly, it seems worthwhile to include here these previously unpublished tables defining this distribution.

In Section II, we arrive at design criteria for an N-vector distribution via the consideration of the phonon spectrum problem and that of averaging over the elastic wave velocities of a crystal to determine its Debye θ_D. But, a vector distribution defined by the set of subsets of direction cosines (p, q, r) has much broader applicability. By permuting (p, q, r), one extends the set from the 1/48th, trihedral angle of Fig. 1a or 1b to the six such segments defining the positive octant. Then, by sign changes, the basic set can be further extended to the full 4π steradians. Thus, the results of Table II can be applied to give accurate three-dimensional spatial integration of many types of functions.

An exactly uniform distribution of the 1/48th trihedral angle of Fig. 1b simply means first dividing the surface area so subtended on the unit sphere into N equal areas. While this seems simple it has nevertheless proven to be a bit tedious. Thus, it seems worthwhile to outline in Section III the straightforward procedures for doing this subdivision. The second step is to find the direction cosines p, q, r of the vector passing through the centroid of each elemental area. This is done in

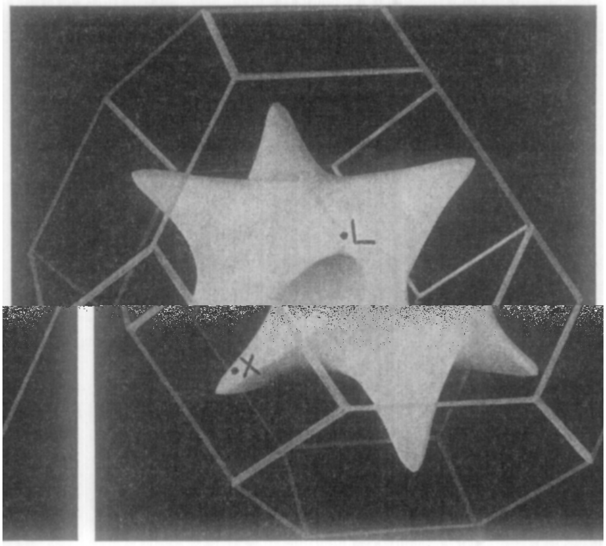

FIG. 2. An anisotropic surface of constant frequency ν_V inside the Brillouin zone of a face-centered cubic lattice which just touches the center L of the hexagonal zone face. The surface becomes sharply conical at L which becomes a saddle point in three dimensions such that nearby surfaces with $\nu > \nu_V$ are hyperbolic while those for $\nu < \nu_V$ are parabolic. Three-dimensional integration to determine $G(\nu)$ is very accurate except near L. A very large increase in $G(\nu)$ occurs close to L as described by Eq. (5.16). Since there is a singularity in $dG/d\nu$ at $\nu = \nu_V$, often with unknown coefficient G_3, the error in $G(\nu_V)$ becomes large and unknown. The square-root singularity occurs for all phonon branches for various ν_V's at X (square face centers), at L, and, in some cases, on symmetry planes.

Section IV. This then completes the design of a uniform N-vector distribution for any N estimated to be large enough to satisfy the accuracy requirements. Our particular results for $N = 489$ are then given in Table II.

Another purpose of this paper is to look at methods of estimating the accuracy of integrations via vectorial methods. One of the methods in Section V is to compare the closed form integrals of certain octahedral functions (the $\mathcal{O}_{n,1,m}$) with corresponding values obtained numerically with an N-489 distribution. Still another method is to do a least-squares polynomial fitting via an independent computer code on the calculated $G(\nu)$ at a number (≈ 50) of ν values of the low-ν range. Here one treats the theoretical $G(\nu)$ points just like experimental data. Theory requires fitting a polynomial of the form $G(\nu) = \sum_n a_n \nu^{2n}$; $\nu < \nu_V$; $\nu_V = \nu$ of lowest Van Hove singularity [1]. When variances of the polynomial fit are of the order of 10^{-10}, one feels assured that $G(\nu)$ has the desired five(or better)-decimal accuracy. Standard deviations of the a_1 for some recent phonon calculations [9] turn out to be of the order of 10^{-5} to 10^{-6}. However, when $\nu > \nu_V$, the errors increase considerably for reasons discussed in Section V.

Spherical surfaces of constant $\nu(\mathbf{q})$ are rarely found in lattice dynamics. Only a very few crystalline solids seem to be almost isotropic in the long wave elastic limit. A typical anisotropic surface of constant frequency is shown in Fig. 2. The causes of error in calculated $G(\nu)$ are considered in Section V and discussed in terms of the anisotropy of the surfaces. We compare in Section VI various integration methods which use interpolations to increase effective point density.

II. Design Considerations

The formal expression for phonon density of states is

$$G(\nu) = (N_0/V_z) \sum_p \int_{S_{\nu_p}} | \nabla_{\mathbf{q}} \nu_p |^{-1} \, dS \tag{2.1}$$

where $G(\nu)\,d\nu$ is the number of crystal vibrations with ν between ν and $\nu + d\nu$, N_0 = Avagadro's number, V_z = Brillouin zone volume in $\mathbf{q}$ space, and p is the index of phonon wave polarization.

For cubic crystals, one can approximate (2.1) by summing over a vector distribution such as that in Fig. 1a or 1b according to

$$g(\nu) = (48 N_0/V_z) \sum_p \sum_{\kappa=1}^{N} q_\kappa^2(\nu_p) \, | dq/d\nu |_{\mathbf{q}=\mathbf{q}(\nu_p)} \, \Delta\omega_\kappa \, . \tag{2.2}$$

When all N elemental solid angle elements are equal, as in Fig. 1b and Table II, $\Delta\omega_\kappa$ can be factored in front of the sum. Both $\nu_p(\mathbf{q})$ and $| dq/d\nu_p |_{\mathbf{q}=\mathbf{q}(\nu)}$ are evaluated along the κth vector by solving (1.1) at several points on $\mathbf{q}_\kappa$; one then uses inverse interpolation to get $\mathbf{q}(\nu_p)$ and the derivative along $\mathbf{q}_\kappa$.

Houston [3] has shown that (2.2) approaches (2.1) with zero error as N in (2.2) $\to \infty$. This procedure, called the vector-interpolation method [5, 9], does not imply interpolation between ν or q values on adjacent vectors.

The solutions of (1.1) can be computed via ordinary machine programs (double precision probably unnecessary) with 10- to 14-decimal accuracy. There is harly any loss of this accuracy in the inverse interpolations which lead to the summand of (2.2). Consequently, virtually all of the error in $g(\nu)$ arises because of the vector distribution. We discover in Section V that this error is relatively large for highly anisotropic surfaces (see Fig. 2). It becomes negligible (order of parts in 10^8) for nearly spherical surfaces.

A choice of N of the order of 500 inside the 1/48th segment of Fig. 1b will provide the desired 5- to 8-decimal accuracy in integrations. This fact was determined in Ref. [7] by a purely geometrical analysis of the errors in evaluating the summand of (2.2). In Ref. [7] we considered the intersection of a surface with an elemental tetrahedral cone of Fig. 1b. Since this analysis corroborates the results of Section V below, we will not repeat it here. The choice of a specific N close to 500 is then arrived at arbitrarily as discussed in Section III.

In the long-wave low temperature limit, the evaluation of (2.2) becomes equivalent to integration over an elastic wave surface. Hence, the problem becomes equivalent to the determination of Debye θ_D. This is discussed further in Section V.

III. Design of a Vector Distribution

In Ref. [7] and in Fig. 1a an elemental tetrahedron defining a $\Delta\omega$ was enclosed by right and left side planes which satisfied the condition ϕ = constant. The upper and lower sides were curves, however, since they satisfied the condition θ = const. This condition on θ could not be extended to elements 60–70 of Fig. 1a because the upper limit θ was defined by a boundary plane of the 1/48 trihedral angle, i.e., the [010]–[101] plane of Figs. 1a and 1b. (Here r, θ, ϕ are spherical coordinates for x, y, z frame of Fig. 1b). This imposed the condition $\theta = \cot^{-1}(\cos\phi)$ as an upper limit of integration. Moreover, the distribution was not uniform because all of the elemental $\Delta\omega_\kappa$ were not equal.

In designing our new higher-density vector distribution, it is convenient to retain the condition ϕ = const for the side planes of each elemental tetrahedron. However, for a uniform distribution, the mathematics becomes tractable only if we use planes for the upper and lower sides instead of the curved sides used in the earlier work. It is convenient to select many planes which intersect in the y- or [010]-axis of Fig. 1a or b. This imposes a condition similar to $\cot\theta = \cos\phi$; in fact, the new condition we seek is $\cot\theta = (\text{const})\cos\phi$.

This section sets down the procedure by which the side planes of each elemental tetrahedron can be so selected that all tetrahedra subtend equal angles and completely fill up the 1/48 basic trihedral angle. The vectors which pass through the centroids of these elemental tetrahedra will then be uniformly distributed.

Figure 1b shows the cuts of a large number of planes on the unit sphere, all of which have a common intercept in the y-axis. Since any pair forms a wedge, we name them wedge planes and label them i with $i = 0, 1, 2, \ldots, L$. Let $i = 0$ be the y–z plane and $i = L$ be the [010]–[101] plane of the figures. Any point $P(x, y, z)$ on the ith plane must satisfy $x = a_i z$ for all x, z. Thus the case $\phi = 0$ (or $y = 0$) defines the line $x^\circ = a_i z^\circ$ as the intercept of the ith plane with the x–z plane of Fig. 1b. Thus for all points on the ith plane, we must have

$$a_i = \tan \theta_i^0, \tag{3.1}$$

where $\theta_i^0 = \theta_i(\phi = 0)$. In View of (3.1), any vector lying in the ith plane will have its θ related to its ϕ according to

$$\theta = \cot^{-1}(\cos \phi / a_i). \tag{3.2}$$

The $i = 0, 1, \ldots, L$ wedge planes cut out L strips on the unit sphere within the 1/48 trihedral angle in the manner shown in Fig. 1b. The edges of these strips are not quite parallel but diverge slightly between the planes $\phi = 0$ (x–z plane) and $\phi = 45°$ (z–[110] plane). We label a strip ℓ with $\ell = 1, 2, 3, \ldots, L$ and ultimately require that each strip shall contain exactly n_ℓ units of elemental solid angle $\Delta\omega = (4\pi/48N)$, where n_ℓ and N are integers to be determined by the aribrary procedure below. The area on a unit sphere between any two planes i, $i + 1$, or the area of the ℓth strip, is given in closed form by

$$A_{i,i+1} = A_\ell = \int_0^{\pi/4} d\phi \int_{\theta_i(\phi)}^{\theta_{i+1}(\phi)} \sin\theta \, d\theta, \tag{3.3}$$

$$= \int_0^{\pi/4} d\phi \left\{ -\cos\left[\cot^{-1}\left(\frac{\cos\phi}{a_{i+1}}\right)\right] + \cos\left[\cot^{-1}\left(\frac{\cos\phi}{a_i}\right)\right]\right\}, \tag{3.4}$$

$$= \left[\sin^{-1}\left(\frac{\sin\phi}{(1 + a_i^2)^{1/2}}\right) - \sin^{-1}\left(\frac{\sin\phi}{(1 + a_{i+1}^2)^{1/2}}\right)\right]\Bigg|_0^{\pi/4}. \tag{3.5}$$

We choose, as a criterion for the determination of n_ℓ and N, a span which may give the 1 part in 10^5 accuracy indicated in Section II. This means choosing $\Delta\theta \approx 1.5°$, $\Delta\phi \approx 1.5°$. Thus, for a preliminary calculation, we arbitrarily put $\Delta\theta^0 \equiv 1.5°$, and this automatically sets a preliminary value of L at 30. The area of these 30 strips can be computed readily by desk calculator; of course, they cannot all contain an integral number of $\Delta\omega$'s. It then becomes necessary to readjust from

$\Delta\theta^0 = 1.5°$ to $\Delta\theta^0 \approx 1.5°$ in order to guarantee $n_\ell \, \Delta\omega$ in each strip, with $n_\ell =$ integer. The next step is to pick $\Delta\phi \approx 1.5°$, again in order to satisfy the accuracy criterion. But in the application of this step we have to realize that the width of an elemental tetrahedron (i.e., the value of $\Delta\phi$) will vary in any strip since the width of each strip diverges slightly. Thus we must single out one of the strips in which to do an initial fitting of n_ℓ. Although the full procedure in this section will apply to any arbitrary accuracy criterion or $(\Delta\theta^0, \Delta\phi)$ or N, it is well illustrated, as follows, by our particular final choices. We have singled out the strip $\ell = L$ (in Fig. 1b this is the strip containing elements $\kappa = 462$ and $\kappa = 489$) and find that one can closely fit $n_L = 28$ elementary $\Delta\omega$'s into this strip with N chosen to be 489. This n_L also gives $\Delta\phi \approx 1.5°$ for element 462 of Fig. 1b. What we wanted was some value of N near 500, and $N = 489$ fills this bill nicely. However, any other N in this vicinity would have been satisfactory also. We fixed upon $N = 489$ because with $n_L = 28$ (i.e., $\Delta\phi_{462} \approx 1.5°$) only a very minor adjustment in $\Delta\theta^0 = \theta_L{}^0 - \theta_{L-1}^0$ from 1.5° was required. The success of this adjustment is seen in Appendix Table I. The next step is then to examine the strip $\ell = (L - 1)$. Note that $\Delta\theta^0 = \theta_{L-1}^0 - \theta_{L-2}^0$ must be readjusted from its preliminary value in order to guarantee $n_{L-1} \, \Delta\omega$ in strip $\ell = (L - 1)$ with n_{L-1} exactly integral, where $\Delta\omega$ is now precisely fixed at $(4\pi/48)(1/489)$ as a result of the adjustments in strip $\ell = L$. We found n_{L-1} could be chosen at 28 or 27 and still not cause $\Delta\theta^0$ to differ greatly from 1.5°. We settled upon $n_{L-1} = 28$ after looking at strips $\ell = L - 2$, $\ell = L - 3$, etc. Continuing this fitting process and recalculating the θ_{i+1}^0, $\theta_i{}^0$ for each strip, we then were able to fit exactly $n_\ell \, \Delta\omega$'s into these strips and thereby completely and uniformly fill up the 1/48 trihedral angle. However, for strip $\ell = 1$ (or $\theta_i{}^0 = \theta_0{}^0 = 0$; $\theta_{i+1}^0 = \theta_1{}^0 = 2.6524°$, see Table I) the readjustments required a final filling of the strip with two elemental trihedral angles (elements $\kappa = 1$ and $\kappa = 2$ of Fig. 1b). This resulted in one less strip (29 instead of 30) than was initially assumed in the preliminary design and thus necessitated a relabeling of the ℓ's. The final results of fitting 489 $\Delta\omega$'s into 29 strips, all of which satisfy $(\theta_{i+1}^0 - \theta_i{}^0) = 1.5°$ within [redacted] way are not sufficiently accurate for the ultimate purpose of computing the $\phi_{\kappa-1}$ and ϕ_κ of the individual $\Delta\omega_\kappa$ and the subsequent centroid coordinates. This is because there is an inadvertent loss of four to six decimals in these calculations, so that we might obtain direction cosines of centroid vectors which were only accurate to two or three significant figures. Consequently, after n_ℓ and N have been fixed by the empirical procedure outlined above, it becomes necessary to recalculate the $\cos\theta_i{}^0$. Fortunately, $\cos\theta_i{}^0$ can now be expressed in closed form and evaluated almost exactly. Of course, this was not possible in the preliminary formulation. The procedure for this precise step follows.

Since the n_ℓ are now fixed, let us consider the total area of all $\Delta\omega$'s from elements $\kappa = 1$, $\kappa = 2, \ldots$, up through and including the final element in the ℓth strip. In Fig. 1b this is only the area on the unit sphere contained between the x–z plane, the z–[110] plane, and the plane labeled $(i + 1)$. Note that the upper limit θ_{i+1}^0 of integration in (3.5) occurs in the form $\cos\theta_{i+1}^0 = (1 + a_{i+1})^{-1/2}$ in view of (3.1). Note also that we are following the convention where i denotes the lower θ_i^0 value of a strip, $i + 1$ the upper so that the ℓth strip corresponds to $i + 1$. Thus, the area of all elements, as discussed above, becomes,

$$\text{Area}(0, i+1) = W_\ell = \sum_{\ell=1}^{i+1} n_\ell \Delta\omega \tag{3.6}$$

where $\Delta\omega$ is now precisely fixed at $(4\pi/48N)$. This area is also given exactly by a revised form of (3.5) in which $a_i = 0(\sim\theta_i^0 = 0)$, e.g.,

$$W_\ell = \pi/4 - \sin^{-1}(\cos\theta_{i+1}^0/\sqrt{2}). \tag{3.7}$$

The inverse of (3.7) is

$$\begin{aligned} \cos\theta_{i+1}^0 &= \sqrt{2}\sin(\pi/4 - W_\ell), \\ &= \cos W_\ell - \sin W_\ell . \end{aligned} \tag{3.8}$$

Since it is easy to calculate W_ℓ to something like 14-decimal accuracy, $\cos\theta_{i+1}^0$ can be readily calculated to 14 decimals directly.

We now consider the further subdivision of a particular strip, say ℓ, into exactly n_ℓ smaller surface elements. Referring to Figs. 1a and b we let $\phi_{\kappa-1}$ denote the plane $\phi = \text{const}$ for the left edge of an elemental tetrahedron, and ϕ_κ denote the right edge. The area of intersection of a single tetrahedron with the unit sphere must be $\Delta\omega$, and this is seen to be equivalent to (3.5) if the upper and lower limits $\phi = 0$ and $\phi = \pi/4$ are replaced by $\phi = \phi_{\kappa-1}$ and $\phi = \phi_\kappa$, respectively. However, this replacement gives an equation with the left side, $\Delta\omega$, known exactly, but with two unknowns, $\phi_{\kappa-1}$ and ϕ_κ in the right side. This is reduced to an equation with only one unknown by holding the lower limit of integration at 0 while the upper limit is set at ϕ_κ. The left side in this case is simply the appropriate integer, say $s_\ell(\kappa)$, times $\Delta\omega$. Thus, this particular revision of (3.5) takes the form

$$s_\ell(\kappa)\,\Delta\omega = \sin^{-1}(\cos\theta_i^0 \sin\phi_\kappa) - \sin^{-1}(\cos\theta_{i+1}^0 \sin\phi_\kappa). \tag{3.9}$$

With the aid of an antitrigonometric identity we express (3.9) in the more convenient form

$$\begin{aligned} &\sin[s_\ell(\kappa)\,\Delta\omega] \\ &\quad = \sin\phi_\kappa[\cos\theta_i^0(1 - \cos^2\theta_{i+1}^0 \sin^2\phi_\kappa)^{1/2} - \cos\theta_{i+1}(1 - \cos^2\theta_i \sin^2\phi_\kappa)^{1/2}]. \end{aligned} \tag{3.10}$$

We are faced at this point with the numerical task of evaluating $\sin \phi_\kappa$ in (3.10) when all the other quantities are known almost exactly, say to 14 decimals. The $\sin \phi_\kappa$ were found for our 489-element subdivision by use of a Newton–Raphson interpolation program. The calculations could be readily checked since, when $s_\ell(\kappa) = n_\ell$, $\phi_\kappa = \pi/4$ and $\sin \phi_\kappa = 1/\sqrt{2}$. (Note the definition of n_ℓ in Table I.) This checked to only 12 decimals, thereby showing that the calculation (3.10) had resulted in a loss of absolute accuracy of two decimals. This is, of course, the consequence of taking the difference in (3.10) of two numbers which are equal to within about 1 percent.

It is not really necessary to retain or print out these $\sin \phi_\kappa$ (we actually did this anyway to check the accuracy of the calculation) since they are used subsequently only to calculate the direction cosines of the centroid vectors by the method of Section 4.

V. Calculation of Centroids

The wedge planes and the planes of constant ϕ cutting out the elemental areas on a unit sphere also define solid angle cones. The solid angles are tetrahedral angles for elements $\kappa = 3$ to 489, and trihedral angles for elements 1 and 2 (note Fig. 1b). We may close these solid angles and form solid figures by any sphere of radius a.

Let $\boldsymbol{\rho}_\kappa$ be the centroid vector of the solid figure defined by the κth tetrahedral (or trihedral) cone. The components of $\boldsymbol{\rho}_\kappa$ are given by well-known formulas which we express in terms of the problem at hand as follows.

$$\begin{aligned}\bar{x}_\kappa &= V_\kappa^{-1} \iiint (\rho \sin \theta \cos \phi)(\rho^2 \sin \theta \, d\rho \, d\theta \, d\phi) \\ &= (a^4/4V_\kappa) \int_{\phi_{\kappa-1}}^{\phi_\kappa} \cos \phi \left\{ \int_{\theta_i(\phi)}^{\theta_{i+1}(\phi)} \sin^2 \theta \, d\theta \right\} d\phi,\end{aligned} \tag{4.1}$$

where $\theta_i(\phi)$ is defined by (3.2) and, ultimately (3.8).

$$\bar{y}_\kappa = (a^4/4V_\kappa) \int_{\phi_{\kappa-1}}^{\phi_\kappa} \sin \phi \left\{ \int_{\theta_i(\phi)}^{\theta_{i+1}(\phi)} \sin^2 \theta \, d\theta \right\} d\phi, \tag{4.2}$$

$$\bar{z}_\kappa = (a^4/4V_\kappa) \int_{\phi_{\kappa-1}}^{\phi_\kappa} \left\{ \int_{\theta_i(\phi)}^{\theta_{i+1}(\phi)} \sin \theta \cos \theta \, d\theta \right\} d\phi. \tag{4.3}$$

The volume of the κth solid figure is

$$V_\kappa = (a^3/3) \int_{\phi_{\kappa-1}}^{\phi_\kappa} \left\{ \int_{\theta_i(\phi)}^{\theta_{i+1}(\phi)} \sin \theta \, d\theta \right\} d\phi, \tag{4.4}$$

which integrates to $(a^3/3)$ times the same result expressed by (3.5) when its limits $\pi/4$ and 0 are replaced by ϕ_κ and $\phi_{\kappa-1}$, respectively. Thus,

$$V_\kappa = (a^3/3)\,\Delta\omega \qquad \text{for all } \kappa. \tag{4.5}$$

Equations (4.1), (4.2), and (4.3) also integrate directly to give, respectively,

$$\begin{aligned}\bar{x}_\kappa = (3a/8\Delta\omega)\Big[&\sin\phi\tan^{-1}\left(\frac{a_{i+1}}{\cos\phi}\right) - \sin\phi\tan^{-1}\left(\frac{a_i}{\cos\phi}\right)\\ &- \frac{1}{(1+a_{i+1}^2)^{1/2}}\tan^{-1}\left(\frac{a_{i+1}\tan\phi}{(1+a_{i+1}^2)^{1/2}}\right)\\ &+ \frac{1}{(1+a_i^2)^{1/2}}\tan^{-1}\left(\frac{a_i\tan\phi}{(1+a_i^2)^{1/2}}\right)\Big]\Big|_{\phi_{\kappa-1}}^{\phi_\kappa},\end{aligned} \tag{4.6}$$

$$\bar{y}_\kappa = (3a/8\Delta\omega)\left[-\cos\phi\tan^{-1}\left(\frac{a_{i+1}}{\cos\phi}\right) + \cos\phi\tan^{-1}\left(\frac{a_i}{\cos\phi}\right)\right]\Big|_{\phi_{\kappa-1}}^{\phi_\kappa}, \tag{4.7}$$

$$\begin{aligned}\bar{z}_\kappa = (3a/8\Delta\omega)\Big[&\frac{a_{i+1}}{(1+a_{i+1}^2)^{1/2}}\tan^{-1}\left(\frac{a_{i+1}\tan\phi}{(1+a_{i+1}^2)^{1/2}}\right)\\ &- \frac{a_i}{(1+a_i^2)^{1/2}}\tan^{-1}\left(\frac{a_i\tan\phi}{(1+a_i^2)^{1/2}}\right)\Big]\Big|_{\phi_{\kappa-1}}^{\phi_\kappa}.\end{aligned} \tag{4.8}$$

The individual parts within the square brackets of (4.6), (4.7), and (4.8) can be calculated to 14-decimal accuracy, but the $\sin\phi$ and $\cos\phi$ going into these parts have only 12-decimal accuracy, as discussed earlier. Note that (4.6) involves four sets of differences; (4.7), two sets; and (4.8), two sets. The numbers in these differences are nearly equal (they differ by only 1 percent), and this results in a further loss of absolute accuracy. Thus the $\bar{x}$, $\bar{y}$, $\bar{z}$, and the direction cosines which we shall ultimately compute from them, can have only about 10-decimal accuracy, even though our computational accuracy is 14 decimals.

Of course, 10-decimal accuracy is just what we wanted in the beginning, since this is all that we shall ever really need in applications. It is interesting to note, however, that we would not have achieved this desired absolute accuracy if we had not required at least 14-decimal accuracy in all steps leading up to these last evaluations.

The desired end product is Table II of the Appendix, e.g., a table of the direction cosines of the 489 vectors passing through the centroids. They are defined by

$$p_\kappa = \bar{x}_\kappa/\rho_\kappa = \sin\bar{\theta}_\kappa\cos\bar{\phi}_\kappa, \tag{4.9}$$

$$q_\kappa = \bar{y}_\kappa/\rho_\kappa = \sin\bar{\theta}_\kappa\sin\bar{\phi}_\kappa, \tag{4.10}$$

$$r_\kappa = \bar{z}_\kappa/\rho_\kappa = \cos\bar{\phi}_\kappa, \tag{4.11}$$

$$\rho_\kappa = (\bar{x}_\kappa{}^2 + \bar{y}_\kappa{}^2 + \bar{z}_\kappa{}^2)^{1/2}. \tag{4.12}$$

V. Accuracy of Spatial Integration

The cubic invariant polynomials mentioned in the introduction are functions of the direction cosines $p(\theta, \phi)$, $q(\theta, \phi)$, $r(\theta, \phi)$. These functions are well suited to provide estimates of the accuracy of integration in terms of the anisotropy of the surfaces. Four of these functions are [8]:

$$\mathcal{O}_{2,2} = p^2q^2 + q^2r^2 + r^2p^2, \tag{5.1}$$

$$\mathcal{O}_{2,2,2} = p^2q^2r^2, \tag{5.2}$$

$$\mathcal{O}_4 = 1 - 2\mathcal{O}_{2,2}, \tag{5.3}$$

$$\mathcal{O}_{4,2} = \mathcal{O}_{2,2} - 3\mathcal{O}_{2,2,2}\,. \tag{5.4}$$

A list of the first 22 polynomials is given in Ref. [8]. One also finds in Ref. [8] three-dimensional sketches of the above four functions which provide an immediate appraisal of the nature of the surface anisotropy.

If one regards the value of $\mathcal{O}_{n,1,m}(\theta, \phi)$ as the length $r(\theta, \phi)$ of a vector from the origin to the surface, then the exact total surface area is given by integration in closed form. One has

$$A_{n,1,m} = \int_0^{2\pi} d\phi \int_0^{\pi} \mathcal{O}_{n,1,m}(\theta, \phi) \sin\theta\, d\theta. \tag{5.5}$$

The surface areas of the functions (5.1) to (5.4) turn out to be

$$\begin{aligned} A_{2,2} &= 4\pi/5 = 2.513274..., \\ A_{2,2,2} &= 4\pi/105 = 0.1196797..., \\ A_4 &= 12\pi/5 = 7.539822..., \\ A_{4,2} &= 24\pi/35 = 2.154235..., \end{aligned} \tag{5.6}$$

respectively.

Using the p, q, r of the 489-vector distribution of Table 2, one has nine-to ten-decimal accuracy for calculated values of the functions (5.1)–(5.4). Using the 13-decimal format deck of p, q, r, one has about 12-decimal accuracy on any given vector. Consequently, any error in integration is largely determined by the coarseness of the subdivision, rather than by numerical errors in the $\mathcal{O}_{n,1,m}(\theta, \phi)$. The numerical estimates of the surface areas are obtained by computer evaluation of

$$E_{n,1,m} = 48\Delta\omega \sum_{\kappa=1}^{489} \mathcal{O}_{n,1,m}(\theta_\kappa \phi_\kappa) \tag{5.7}$$

The results obtained via the $N = 489$ distribution of Table II are:

$$\begin{aligned} E_{2,2} &= 2.513366 \text{ (high by 3.6 parts in } 10^5), \\ E_{2,2,2} &= 0.1196624 \text{ (low by 14.4 parts in } 10^5), \\ E_4 &= 7.539639 \text{ (low by 2.4 parts in } 10^5), \\ E_{4,2} &= 2.154378 \text{ (high by 6.6 parts in } 10^5). \end{aligned} \tag{5.8}$$

One gauge of the surface anisotropy of the $\mathcal{O}_{n,1,m}$ obtains by recording the length of a vector from the origin to the surface in the [001] (z-axis), [101] (face-diagonal), and [111] (body diagonal) directions. This length is simply the value of $\mathcal{O}_{n,1,m}$ in the direction of interest. One finds,

$$\begin{aligned} \mathcal{O}_{2,2} &= 0;\ 1/4;\ 1/3, \\ \mathcal{O}_{2,2,2} &= 0;\ 0;\ 1/27, \\ \mathcal{O}_4 &= 1;\ 1/2;\ 1/3, \\ \mathcal{O}_{4,2} &= 0;\ 1/4;\ 2/9, \end{aligned} \tag{5.9}$$

in the [001], [101], and [111] directions, respectively.

Comparing (5.9) with numerical results (5.8) leads one to at least a qualitative relationship between surface anisotropy and error of numerical integration. The very coarse 70-vector subdivision [5] of Fig. 1a has errors of several percent for surfaces like $\mathcal{O}_{2,2,2}$ and less than one percent for $\mathcal{O}_{2,2}$ and $\mathcal{O}_{4,2}$. For $\mathcal{O}_4$, the error is less than one part in 10^3; thus even crude subdivisions can give satisfactory results (for certain purposes) if the anisotropy is known not to be too great.

Elastic wave surfaces in crystals have anisotropies more closely like that of $\mathcal{O}_4$. See (5.9). One seldom finds anything as anisotropic as $\mathcal{O}_{2,2,2}$. Generally, the longitudinal and high-shear wave velocity surfaces are less-anisotropic than $\mathcal{O}_4$ while the low-shear mode is about like $\mathcal{O}_4$.

In some high-transition-temperature superconductors, the high T_c is attributed to the existence of soft phonon modes, i.e., a very small velocity of the low-shear mode in a certain crystallographic direction (say the [110]-direction in cubic metals). In such a case, the surface of constant ν becomes quite anisotropic so that errors of integration by our vector technique become larger. We can expect errors perhaps as large as 6 parts in 10^5, such as those for $\mathcal{O}_{2,2}$ and $\mathcal{O}_{4,2}$ in (5.8).

In computing tables of Debye θ_D functions, one goes to the long-wave limit of Eq. (2.2). Restricting ourselves to the case of all cubic crystals, one puts (2.2) into the expression for the specific heat [4], then goes over to the long wave limit. In the low ν power series for $G(\nu) = \sum_n a_n \nu^{2n}$, only the coefficient a_1 remains significant in the long-wave, low-ν, low-temperature limit. One finds a result [4, 10] in terms of the cubic crystal elastic wave velocities according to

$$\theta_D = \left(\frac{h}{k}\right)\left(\frac{9N_0}{4\pi V}\right)^{1/2} \left(\frac{9}{18+3}\right)^{1/3} \left(\frac{c_{44}}{\rho}\right)^{1/3} G(S, \tau), \tag{5.10}$$

$$G(s, \tau) = \left\{\frac{9}{18+\sqrt{3}} \frac{1}{N} \sum_{p=1}^{3} \sum_{\kappa=1}^{N} [1 + \tau U_\kappa(S, \theta_\kappa, \phi_\kappa)]^{-3/2}\right\}^{-1/3} \tag{5.11}$$

where c_{11}, c_{12}, c_{44} are the elastic constants and the dimensionless parameters are

$$S = (c_{11} - c_{44})/(c_{12} + c_{44}), \tag{5.12}$$

$$\tau = (c_{12} + c_{44})/c_{44}, \tag{5.13}$$

and V = crystal molar volume.

There are only three elastic modes in cubics so $p = 1, 2, 3$ and κ extends over all N vectors of the distribution in the 1/48th trihedral angle. The function

$$U = \frac{1}{\tau} [\rho v_p^2(\theta_\kappa, \phi_\kappa) - 1] \tag{5.14}$$

is a reduced form of the pth root of the elastic secular equation (v_p = velocity of pth mode). It turns out that $U = U(S, \theta_\kappa, \phi_\kappa) = U[S, \mathcal{O}_{2,2}(\kappa), \mathcal{O}_{2,2,2}(\kappa)]$, i.e., it is a root of the cubic

$$U^3 - U^2S + U(S^2 - 1)\, \mathcal{O}_{2,2} - (S^3 - 3S + 2)\, \mathcal{O}_{2,2,2} = 0, \tag{5.15}$$

However, $1 + \tau U$ is seldom as anisotropic as either $\mathcal{O}_{2,2}$ or $\mathcal{O}_{2,2,2}$ except perhaps in the soft-phonon-mode case already discussed.

We have evaluated [10] six-decimal tables of the function $G(s, \tau)$ characterized by $0.04 \leqslant S \leqslant 7.51$ ($\Delta S = 0.03$) and $1.00 \leqslant \tau \leqslant 4.80$ ($\Delta\tau = 0.05$). This range covers virtually all of the values for existing experimental data on the elastic constants c_{11}, c_{12}, c_{44} of cubic crystals. By interpolation, we evaluate $G(S, \tau)$ rapidly and with about six-decimal accuracy. Thus, one can obtain from the tables of Ref. [10] an accurate θ_D for essentially all of the known sets of cubic crystal elastic constants. The question then is, just how accurate is it?

We get an immediate answer by comparing with data on phonon spectra in Ref. [9]. There, the standard deviation of the quadratic coefficient a_1 (which determines θ_D) obtained from least squares adjustment of $G(\nu)$ versus ν was 7×10^{-6}. This was for the case of copper. The much simpler calculations via (5.15) are expected to be more accurate but, as already pointed out, the roughness of the vector distribution is the main factor in determining accuracy. However, from this result we can claim 7 parts in 10^6, at least, as the accuracy of θ_D calculations via the tables of Ref. [10] when the (S, τ) range is more isotropic than that for copper.

Compare now with the anisotropy indicated by (5.9). The Debye velocity surface obtained from the roots of (5.15) is not, for any of the p roots, as anisotropic as the functions of Eq. (5.9). The worst case would be like $\mathcal{O}_4$ and should be off by only about 2.4 parts in 10^5. Consequently, for the location of (S, τ) in the θ_D tables of Ref. [10], the accuracy is at least as good as 7 parts in 10^6. For the more-isotropic cases of these tables, the accuracy is much better. But, the top edge of these tables corresponds to (S, τ) values at which the roots of (5.15) become complex. There, the anisotropy is also large, but seldom as bad as $\mathcal{O}_{2,2}$ in (5.9). The worst conceivable case is the most anisotropic case of $\mathcal{O}_{2,2,2}$, the error of which, in (5.8), is 1.4 parts in 10^4.

The surface of constant frequency $\nu = \nu_V$ shown in Fig. 2 touches the centers of hexagonal faces of the fcc Brillouin zone. At the point of contact $\partial\nu/\partial q$ vanishes in all directions. Thus, one has a saddle point in three dimensions. It has been shown [1] that $G(\nu)$ has a square root singularity, i.e.

$$G(\nu) = G_1 - G_2(\nu_V^2 - \nu^2)^{1/2};\ \nu < \nu_V, \tag{5.16}$$

so that $(\partial G/\partial\nu)|_{\nu=\nu_V}$ is infinite. This is the so-called Van Hove singularity [1 and references cited therein].

The value of G_1 can be estimated with better than one percent accuracy by the use of the method of (2.2) when $\nu \geqslant \nu_V$. When $\nu < \nu_V$ by a few percent the accuracy of $G(\nu)$ is of order of a part in 10^4 to 10^6 as already discussed. Use of these results in combination with G_1 and (5.16) permits an estimate of $G(\nu_V)$ the error of which is about the same as the error of G_1. Often we obtain G_1 with 0.1 percent accuracy but the error is sometimes as large as one percent. Thus, an important feature of the vector method is this capability of estimating the error with some degree of confidence.

VI. Comparison with Other Methods

A further discussion of certain sources of errors in calculations of $G(\nu)$ by our method is presented here rather than in Section V above. This is done here in order to make a more-meaningful comparison with the method of Gilat and Raubenheimer [12] (GR method), the QUAD scheme of Mueller, Garland, Cohen and Bennemann [13] (MGCB), and a Monte Carlo method of Brust [14]. While many other authors (see Refs. cited in [7, 12, 13, 14]) have devised integration

TABLE IIA (*continued*)

k	p_k	q_k	r_k
135	.35364 83310	.29616 45992	.88725 38465
136	.35120 83166	.31658 53880	.88115 06173
137	.34858 71405	.33700 54130	.87459 38240
138	.39452 37167	.01019 48516	.91882 92017
139	.39435 92378	.03058 45268	.91844 72648
140	.39403 00779	.05097 41181	.91768 29174
141	.39353 58315	.07136 35702	.91653 52095
142	.39287 58870	.09175 28287	.91500 27081
143	.39204 94228	.11214 18401	.91308 34889
144	.39105 54024	.13253 05528	.91077 51231
145	.38989 25669	.15291 89168	.90807 46617
146	.38855 94269	.17330 68842	.90497 86161
147	.38705 42528	.19369 44099	.90148 29344
148	.38537 50620	.21408 14516	.89758 29731
149	.38351 96056	.23446 79701	.89327 34649
150	.38148 53516	.25485 39299	.88854 84798
151	.37926 94661	.27523 92992	.88340 13812
152	.37686 87913	.29562 40507	.87782 47745
153	.37427 98202	.31600 81617	.87181 04484
154	.37149 86675	.33639 16142	.86534 93063
155	.36852 10360	.35677 43959	.85843 12881
156	.41855 12610	.01016 09759	.90813 63315
157	.41837 79773	.03048 29035	.90776 13457
158	.41803 11980	.05080 47585	.90701 09117
159	.41751 04978	.07112 64928	.90588 41020
160	.41681 52355	.09144 80592	.90437 95176
161	.41594 45496	.11176 94116	.90249 52799
162	.41489 73532	.13209 05051	.90022 90180
163	.41367 23265	.15241 12962	.89757 78535
164	.41226 79087	.17273 17436	.89453 83817
165	.41068 22864	.19305 18081	.89110 66485
166	.40891 33826	.21337 14529	.88727 81236
167	.40695 88406	.23369 06439	.88304 76686
168	.40481 60083	.25400 93505	.87840 94998
169	.40248 19178	.27432 75449	.87335 71457
170	.39995 32625	.29464 52033	.86788 33977
171	.39722 63716	.31496 23058	.86198 02525
172	.39429 71792	.33527 88370	.85563 88467
173	.39116 11900	.35559 47857	.84884 93811
174	.38781 34385	.37591 01460	.84160 10332
175	.44238 29338	.01011 46408	.89676 92200
176	.44220 14976	.03034 39011	.89640 22998
177	.44183 84050	.05057 30983	.89566 80108
178	.44129 32139	.07080 21903	.89456 54527
179	.44056 52580	.09103 11362	.89309 32682
180	.43965 36422	.11125 98957	.89124 96342
181	.43855 72372	.13148 84296	.88903 22506
182	.43727 46720	.15171 67002	.88643 83251
183	.43580 43251	.17194 46713	.88346 45551
184	.43414 43138	.19217 23088	.88010 71063
185	.43229 24809	.21239 95806	.87636 15859
186	.43024 63804	.23262 64569	.87222 30126
187	.42800 32597	.25285 29108	.86768 57814
188	.42556 00394	.27307 89181	.86274 36221
189	.42291 32900	.29330 44579	.85738 95521
190	.42005 92054	.31352 95127	.85161 58222
191	.41699 35712	.33375 40687	.84541 38532
192	.41371 17300	.35397 81163	.83877 41637
193	.41020 85394	.37420 16498	.83168 62867
194	.40647 83250	.39442 46683	.82413 86730
195	.46602 58234	.01005 78944	.88471 39485
196	.46583 68706	.03017 36648	.88435 60143
197	.46545 87378	.05028 93799	.88363 97126
198	.46489 09692	.07040 50031	.88256 41746
199	.46413 28779	.09052 04984	.88112 80900
200	.46318 35408	.11063 58308	.87932 96995
201	.46204 17939	.13075 09659	.87716 67832
202	.46070 62241	.15086 58706	.87463 66469
203	.45917 51602	.17098 05134	.87173 61047
204	.45744 66622	.19109 48643	.86846 14580
205	.45551 85082	.21120 88951	.86480 84709
206	.45338 81792	.23132 25797	.86077 23411
207	.45105 28410	.25143 58943	.85634 76663
208	.44850 93244	.27154 88179	.85152 84055
209	.44575 41011	.29166 13317	.84630 78334
210	.44278 32564	.31177 34205	.84067 84892
211	.43959 24582	.33188 50718	.83463 21164
212	.43617 69208	.35199 62770	.82815 95950
213	.43253 13631	.37210 70308	.82125 08615
214	.42864 99608	.39221 73322	.81389 48184
215	.42452 62910	.41232 71841	.80607 92278
216	.48894 99197	.01045 90707	.87224 91524
217	.48873 56034	.03137 71951	.87186 75253
218	.48830 66915	.05229 52688	.87110 37710
219	.48766 26236	.07321 32584	.86995 68865
220	.48680 25547	.09413 11311	.86842 53583
221	.48572 53490	.11504 88546	.86650 71531
222	.48442 95725	.13596 63979	.86419 97037
223	.48291 34834	.15688 37311	.86149 98912
224	.48117 50191	.17780 08255	.85840 40234
225	.47921 17826	.19871 76544	.85490 78086
226	.47702 10240	.21963 41927	.85100 63243
227	.47459 96207	.24055 04176	.84669 39805
228	.47194 40531	.26146 63083	.84196 44769
229	.46905 03768	.28238 18469	.83681 07531
230	.46591 41902	.30329 70182	.83122 49311
231	.46253 05976	.32421 18098	.82519 82481
232	.45889 41652	.34512 62128	.81872 09796
233	.45499 88715	.36604 02218	.81178 23495
234	.45083 80491	.38695 38350	.80437 04265
235	.44640 43167	.40786 70550	.79647 20029
236	.44168 95006	.42877 98884	.78807 24537
237	.51123 39620	.01034 60231	.85937 93085
238	.51101 47256	.03103 80543	.85901 14024
239	.51057 59732	.05173 00408	.85827 51182
240	.50991 71434	.07242 19533	.85716 95092
241	.50903 73898	.09311 37626	.85569 31477
242	.50793 55751	.11380 54404	.85384 41153
243	.50661 02637	.13449 69594	.85161 99908
244	.50505 97120	.15518 82929	.84901 78332
245	.50328 18565	.17587 94158	.84603 41624
246	.50127 42997	.19657 03043	.84266 49345
247	.49903 42926	.21726 09361	.83890 55134
248	.49655 87148	.23795 12909	.83475 06370
249	.49384 40516	.25864 13502	.83019 43776
250	.49088 63663	.27933 10979	.82523 00971
251	.48768 12693	.30002 05202	.81985 03931
252	.48422 38813	.32070 96059	.81404 70388
253	.48050 87923	.34139 83466	.80781 09120
254	.47653 00120	.36208 67370	.80113 19133
255	.47228 09147	.38277 47751	.79399 88723
256	.46775 41734	.40346 24623	.78639 94372
257	.46294 16844	.42414 98039	.77831 99475
258	.45783 44786	.44483 68090	.76974 52849
259	.53341 95587	.01023 20717	.84578 89093
260	.53319 58465	.03069 62020	.84543 47594
261	.53274 81427	.05116 02929	.84472 60152
262	.53207 58868	.07162 43183	.84366 17851
263	.53117 82335	.09208 82525	.84224 07245
264	.53005 40474	.11255 20706	.84046 10272
265	.52870 18954	.13301 57483	.83832 04140
266	.52712 00378	.15347 92620	.83581 61173
267	.52530 64160	.17394 25894	.83294 48631
268	.52325 86392	.19440 57093	.82970 28485
269	.52097 39673	.21486 86021	.82608 57154
270	.51844 92918	.23533 12494	.82208 85201
271	.51568 11129	.25579 36349	.81770 56965
272	.51266 55136	.27625 57439	.81293 10150
273	.50939 81287	.29671 75640	.80775 75340
274	.50587 41102	.31717 90849	.80217 75444
275	.50208 80870	.33764 02989	.79618 25051
276	.49803 41177	.35810 12007	.78976 29693
277	.49370 56370	.37856 17880	.78290 84983
278	.48909 53930	.39902 20616	.77560 75624

TABLE IIA (*continued*)

k	p	q	r
[illegible]	[illegible]	[illegible]	[illegible]
282	.55548 73439	.01011 72035	.83146 34405
283	.55525 96027	.03035 15990	.83112 30679
284	.55480 38419	.05058 59595	.83044 19051
285	.55411 95035	.07082 02620	.82941 91138
286	.55320 57457	.09105 44839	.82805 34306
287	.55206 14382	.11128 86030	.82634 31583
288	.55068 51547	.13152 25976	.82428 61558
289	.54907 51641	.15175 64471	.82187 98239
290	.54722 94186	.17199 01314	.81912 10888
291	.54514 55410	.19222 36318	.81600 63814
292	.54282 08080	.21245 69306	.81253 16136
293	.54025 21314	.23269 00117	.80869 21497
294	.53743 60365	.25292 28601	.80448 27739
295	.53436 86365	.27315 54628	.79989 76519
296	.53104 56031	.29338 78085	.79493 02870
297	.52746 21330	.31361 98877	.78957 34698
298	.52361 29086	.33385 16933	.78381 92195
299	.51949 20535	.35408 32201	.77765 87166
300	.51509 30806	.37431 44657	.77108 22259
301	.51040 88320	.39454 54302	.76407 90062
302	.50543 14105	.41477 61164	.75663 72067
303	.50015 20979	.43500 65303	.74874 37463
304	.49456 12618	.45523 66810	.74038 41723
305	.48864 82451	.47546 65810	.73154 24956
306	.57741 68552	.01000 14437	.81638 82327
307	.57718 55321	.03000 43209	.81606 16412
308	.57672 26096	.05000 71671	.81540 80665
309	.57602 75333	.07000 99619	.81442 67224
310	.57509 94675	.09001 26853	.81311 64240
311	.57393 72899	.11001 53174	.81147 55801
312	.57253 95850	.13001 78391	.80950 21835
313	.57090 46347	.15002 02320	.80719 37983
314	.56903 04080	.17002 24783	.80454 75447
315	.56691 45472	.19002 45613	.80156 00803
316	.56455 43531	.21002 64653	.79822 75780
317	.56194 67664	.23002 81755	.79454 57005
318	.55908 83464	.25002 96789	.79050 95702
319	.55597 52469	.27003 09635	.78611 37345
320	.55260 31879	.29003 20190	.78135 21259
321	.54896 74229	.31003 28368	.77621 80162
322	.54506 27018	.33003 34101	.77070 39635
323	.54088 32278	.35003 37342	.76480 17513
324	.53642 26083	.37003 38064	.75850 23187
325	.53167 37972	.39003 36262	.75179 56796
326	.52662 90295	.41003 31958	.74467 08290
327	.52127 97447	.43003 25196	.73711 56353
328	.51561 64974	.45003 16053	.72911 67135
329	.50962 88534	.47003 04631	.72065 92784
330	.50330 52678	.49002 91068	.71172 69714
331	.59876 74116	.01027 49870	.80085 70481
332	.59851 42667	.03082 49515	.80051 88910
333	.59800 76575	.05137 48877	.79984 21485
334	.59724 69428	.07192 47766	.79882 59609
335	.59623 11559	.09247 46000	.79746 90320
336	.59495 89983	.11302 43398	.79576 96205
337	.59342 88308	.13357 39784	.79372 55288
338	.59163 86634	.15412 34991	.79133 40881
339	.58958 61410	.17467 28859	.78859 21413
340	.58726 85283	.19522 21234	.78549 60205
341	.58468 26899	.21577 11977	.78204 15221
342	.58182 50685	.23632 00958	.77822 38765
343	.57869 16580	.25686 88060	.77403 77132
344	.57527 79740	.27741 73180	.76947 70200
345	.57157 90183	.29796 56230	.76453 50963
346	.56758 92383	.31851 37140	.75920 44985
347	.56330 24806	.33906 15859	.75347 69780
348	.55871 19366	.35960 92353	.74734 34082
349	.55381 00804	.38015 66611	.74079 37013
350	.54858 85960	.40070 38644	.73381 67110
351	.54303 82933	.42125 08490	.72640 01199

k	p	q	r
[illegible]	[illegible]	[illegible]	[illegible]
355	.51732 84979	.50343 67687	.69204 23723
356	.61917 45279	.01052 93258	.78518 28050
357	.61889 96632	.03158 79685	.78483 46368
358	.61834 95692	.05264 65852	.78413 78370
359	.61752 35141	.07370 51586	.78309 14756
360	.61642 03943	.09476 36717	.78169 41499
361	.61503 87266	.11582 21081	.77994 39750
362	.61337 66382	.13688 04518	.77783 85704
363	.61143 18536	.15793 86874	.77537 50444
364	.60920 16785	.17899 68004	.77254 99727
365	.60668 29806	.20005 47772	.76935 93745
366	.60387 21663	.22111 26049	.76579 86829
367	.60076 51535	.24217 02722	.76186 27105
368	.59735 73402	.26322 77687	.75754 56091
369	.59364 35676	.28428 50856	.75284 08230
370	.58961 80769	.30534 22156	.74774 10345
371	.58527 44602	.32639 91531	.74223 81014
372	.58060 56027	.34745 58940	.73632 29834
373	.57560 36163	.36851 24367	.72998 56580
374	.57025 97621	.38956 87814	.72321 50222
375	.56456 43601	.41062 49306	.71599 87777
376	.55850 66840	.43168 08894	.70832 32974
377	.55207 48373	.45273 66657	.70017 34682
378	.54525 56076	.47379 22701	.69153 25063
379	.53803 42941	.49484 77166	.68238 17376
380	.53039 45018	.51590 30225	.67270 03373
381	.63909 97416	.01035 67132	.76905 41326
382	.63882 52735	.03107 01317	.76872 42138
383	.63827 59850	.05178 35270	.76806 39513
384	.63745 11691	.07249 68837	.76707 24926
385	.63634 97596	.09321 01865	.76574 85518
386	.63497 03241	.11392 34209	.76409 04015
387	.63331 10544	.13463 65724	.76209 58613
388	.63136 97545	.15534 96273	.75976 22828
389	.62914 38257	.17606 25726	.75708 65321
390	.62663 02480	.19677 53960	.75406 49679
391	.62382 55596	.21748 80859	.75069 34153
392	.62072 58307	.23820 06319	.74696 71359
393	.61732 66350	.25891 30246	.74288 07922
394	.61362 30149	.27962 52558	.73842 84068
395	.60960 94425	.30033 73186	.73360 33143
396	.60527 97736	.32104 92077	.72839 81067
397	.60062 71954	.34176 09192	.72280 45699
398	.59564 41648	.36247 24508	.71681 36099
399	.59032 23382	.38318 38022	.71041 51679
400	.58465 24892	.40389 49751	.70359 81210
401	.57862 44131	.42460 59733	.69635 01676
402	.57222 68151	.44531 68028	.68865 76924
403	.56544 71788	.46602 74723	.68050 56084
404	.55827 16124	.48673 79931	.67187 71710
405	.55068 46645	.50744 83795	.66275 37570
406	.54266 91061	.52815 86491	.65311 46014
407	.65892 34696	.01018 98060	.75214 09636
408	.65864 95507	.03056 94112	.75182 86244
409	.65810 13724	.05094 89955	.75120 35566
410	.65727 82518	.07132 85454	.75026 49788
411	.65617 91586	.09170 80472	.74901 17127
412	.65480 27096	.11208 74879	.74744 21760
413	.65314 71590	.13246 68545	.74555 43717
414	.65121 03873	.15284 61348	.74334 58754
415	.64898 98875	.17322 53170	.74081 38197
416	.64648 27482	.19360 43900	.73795 48742
417	.64368 56335	.21398 33435	.73476 52236
418	.64059 47599	.23436 21679	.73124 05403
419	.63720 58688	.25474 08546	.72737 59535
420	.63351 41949	.27511 93961	.72316 60133
421	.62951 44300	.29549 77861	.71860 46485
422	.62520 06807	.31587 60192	.71368 51192
423	.62056 64198	.33625 40917	.70839 99608
424	.61560 44304	.35663 20012	.70274 09202

TABLE IIA (*continued*)

k	p_k	q_k	r_k
425	.61030 67414	.37700 97469	.69669 88819
426	.60466 45522	.39738 73297	.69026 37826
427	.59866 81460	.41776 47523	.68342 45113
428	.59230 67888	.43814 20194	.67616 87946
429	.58556 86106	.45851 91380	.66848 30606
430	.57844 04671	.47889 61171	.66035 22810
431	.57090 77752	.49927 29687	.65175 97832
432	.56295 43189	.51964 97071	.64268 70286
433	.55456 20172	.54002 63501	.63311 33471
434	.67861 10131	.01002 78125	.73442 93947
435	.67833 78226	.03008 34312	.73413 40379
436	.67779 11128	.05013 90313	.73354 29674
437	.67697 02236	.07019 46007	.73265 54677
438	.67587 41604	.09025 01271	.73147 04600
439	.67450 15872	.11030 55989	.72998 64956
440	.67285 08189	.13036 10046	.72820 17468
441	.67091 98103	.15041 63330	.72611 39958
442	.66870 61433	.17047 15737	.72372 06205
443	.66620 70112	.19052 67166	.72101 85770
444	.66341 92002	.21058 17524	.71800 43804
445	.66033 90675	.23063 66724	.71467 40804
446	.65696 25160	.25069 14688	.71102 32345
447	.65328 49654	.27074 61347	.70704 68758
448	.64930 13178	.29080 06640	.70273 94770
449	.64500 59197	.31085 50519	.69809 49078
450	.64039 25165	.33090 92946	.69310 63869
451	.63545 42017	.35096 33897	.68776 64260
452	.63018 33571	.37101 73359	.68206 67658
453	.62457 15849	.39107 11336	.67599 83017
454	.61860 96282	.41112 47846	.66955 09984
455	.61228 72794	.43117 82926	.66271 37900
456	.60559 32732	.45123 16630	.65547 44647
457	.59851 51613	.47128 49032	.64781 95287
458	.59103 91660	.49133 80228	.63973 40476
459	.58315 00061	.51139 10338	.63120 14583
460	.57483 06913	.53144 39509	.62220 33457
461	.56606 22759	.55149 67915	.61271 91761
462	.69778 98676	.01021 92960	.71622 96186
463	.69749 81440	.03065 78824	.71593 04668
464	.69691 43317	.05109 64517	.71533 17879
465	.69603 76986	.07153 49929	.71443 28289
466	.69486 71403	.09197 34947	.71323 24541
467	.69340 11737	.11241 19465	.71172 91385
468	.69163 79271	.13285 03378	.70992 09572
469	.68957 51281	.15328 86585	.70780 55735
470	.68721 00884	.17372 68990	.70538 02230
471	.68453 96858	.19416 50504	.70264 16952
472	.68156 03427	.21460 31041	.69958 63113
473	.67826 80009	.23504 10524	.69620 98984
474	.67465 80919	.25547 88886	.69250 77592
475	.67072 55034	.27591 66064	.68847 46367
476	.66646 45391	.29635 42008	.68410 46745
477	.66186 88741	.31679 16677	.67939 13693
478	.65693 15018	.33722 90043	.67432 75173
479	.65164 46735	.35766 62087	.66890 51522
480	.64599 98287	.37810 32808	.66311 54729
481	.63998 75136	.39854 02215	.65694 87607
482	.63359 72876	.41897 70336	.65039 42823
483	.62681 76129	.43941 37214	.64344 01772
484	.61963 57267	.45985 02914	.63607 33258
485	.61203 74902	.48028 67516	.62827 91950
486	.60400 72109	.50072 31128	.62004 16547
487	.59552 74308	.52115 93879	.61134 27611
488	.58657 86740	.54159 55927	.60216 24973
489	.57713 91429	.56203 17462	.59247 84604

table becomes a useful guide to others who wish to produce a distribution with a different value of N. (b) If one does not wish to go to the trouble to design his own distribution and is content to use our work as a computational aid, then the results of Table IIA can be transcribed onto IBM cards and used directly.

The first column of Table IA identifies the wedge planes of Fig. 1b. The strips cut out by these planes on the unit sphere are labeled by ℓ; thus ℓ in Table IA is shown between the upper wedge plane label $i + 1$ and the lower plane label i. The elements in each strip are numbered consecutively from left to right as indicated in Fig. 1b. Strip $\ell = 1$ contains elements $\kappa = 1, 2$; strip $\ell = 2$ contains $\kappa = 3, 4, 5$; strip $\ell = 3$ contains $\kappa = 6, 7, 8, 9, 10$; etc. Integer n_ℓ counts the number of elements in each strip while $n_\ell \Delta\omega$ is just the area on a unit sphere subtended by the entire strip labeled ℓ. The two $\cos\theta^\circ$ values corresponding to each strip ℓ are located in Table 1A above and below each strip ℓ as shown. As in Eq. (3.6) and elsewhere we use the convention that the lower plane defining strip ℓ be labeled by θ_i^0 while the upper carries the label θ_{i+1}^0, such that $\ell = i + 1$. Table IA shows this convention at a glance. Note that we show only five significant figures in $n_\ell \Delta\omega$, in the $\cos\theta_i^0$ values, and in $\theta_{i+1}^0 - \theta_i^0$. This is sufficient for tabular purposes. Recall, however, that in the text we have stated that both $n_\ell \Delta\omega$ and $\cos\theta_i^0$ have to be known in the calculations to 14 significant figures in order to achieve the final accuracy of only 10 decimals in the p_κ, q_κ, r_κ of Table IIA. Note that κ labels also the polar coordinate angle ϕ_κ corresponding to the right-hand edge (see Fig. 1b) of each surface element.

The elemental solid angle cones formed by the bounding planes defined in Section III and by the labels of Table IA form a solid figure when closed by a unit sphere. The vector passing through the centroid of an elemental cone is labeled by κ just as κ also labels the right edge plane and ϕ_κ of that element. The direction cosines of this centroid vector are p_κ, q_κ, r_κ according to their definitions in Eqs. (4.9) to (4.12). These direction cosines along with the identifying label κ are given in Table IIA.

References

1. A. A. Maradudin, E. W. Montroll, and G. H. Weiss, Solid State Physics (F. Seitz and D. Turnbull, Eds.), Supplement Vol. 3, Academic Press, New York, 1963.
2. G. L. Squires, *Arkiv Fysik* **25** (1963), 21; **26** (1963), 223.
3. W. V. Houston, *Revs. Modern Phys.* **20** (1948), 161.
4. J. de Launay, Solid State Physics (F. Seitz and D. Turnbull, Eds.), Vol. II, Academic Press, New York, (1956).
5. W. C. Overton, Jr., and E. Dent, U. S. Naval Research Laboratory Report No. 5252, Mar. 1959.
6. W. C. Overton, Jr., Proceedings of the VIII International Conference on Low Temperature Physics, p. 677, Univ. of Toronto Press, 1961.

7. W. C. OVERTON, JR., AND A. F. SCHUCH, Los Alamos Scientific Laboratory Report No. LA-3162, Jan. 1965.
8. J. DE LAUNAY, *J. Chem. Physics* **26** (1957), 663 (see also F. C. VON DER LAGE AND H. A. BETHE; *Phys. Rev.* **71** (1947), 612).
9. T. F. STROMBERG, R. J. BALESTRI, AND W. C. OVERTON, JR., *J. Chem. Phys.* **57** (1972), 1502.
10. W. C. OVERTON, JR., AND A. F. SCHUCH, Los Alamos Scientific Laboratory Report No. LA-3615-MS, Dec., 1966; Supplement to LA-3615-MS, Jan., 1967.
11. R. B. LEIGHTON, *Revs. Modern Phys.* **20** (1948), 165.
12. G. GILAT AND R. RAUBENHEIMER, *Phys. Rev.* **144** (1966), 390.
13. F. M. MUELLER, J. W. GARLAND, M. H. COHEN, AND K. H. BENNEMANN, *Ann. Phys.* **67** (1971), 19-57.
14. D. BRUST, *Phys. Rev.* **134** (1964), A1337.
15. G. GILAT AND F. HERMAN, *Ann. Phys.* **67** (1971), 432.
16. D. J. ERICKSON, private communication. (The LASL CDC-6600 Central processor (CP), peripheral processor (PP), and input-output (SS) times were 71,20,20 seconds, respectively, of computer time, which adds up to 91 sec referred to in text. Corresponding CP, PP, SS times for our vector method were 230,20,20 sec respectively. If we compare just CP time, our method takes 230/71 = 3.3 times longer than GR on a 6600 for (51,345/5900)(= 8.7) ratio of matrix diagonalizations. Assuming matrix diagonalizations take the same time per unit, we are left with the conclusion that three-dimensional linear interpolation takes a lot more time per histogram point than one-dimensional fifth-order interpolations.)